

A Computational Attractive Interval Power Flow Approach With Correlated Uncertain Power Injections

Bi Liu¹, Qi Huang¹, *Senior Member, IEEE*, Junbo Zhao², *Member, IEEE*,
and Weihao Hu¹, *Senior Member, IEEE*

Abstract—This paper presents a new computational attractive interval power flow (PF) approach with correlated uncertain power injections while maintaining high estimation accuracy. The key idea is to integrate the ellipsoid convex model with the evidence theory. This allows us to effectively account for uncertain power injection correlations and eliminate irrelevant focal elements, yielding significantly improved computational efficiency. Extensive comparisons with other approaches demonstrate its effectiveness under various conditions.

Index Terms—Power flow, uncertainty, correlations, non-probabilistic convex model, evidence theory.

I. INTRODUCTION

DU E to the uncertainties of distributed energy resources and prosumers, the traditional deterministic power flow may yield incorrect contingency analysis results. The uncertainties of these sources are typically complex and the accurate knowledge of its associated probability distributions are challenging, thus, the probabilistic power flow may not be appropriate to quantify the induced uncertainties. Hence, the interval power flow has been proposed. This is achieved by optimization algorithm [1], [2]–based and analytical-based methods, via affine arithmetic and moment estimate method, [3], [4]. For example, the evidence theory is used with the extended affine arithmetic to calculate the interval power flow [5]. The structural dependences among power injections are taken into consideration as well. In this paper, we propose to integrate the ellipsoid convex model with the evidence theory for interval power flow considering power injection correlations. It achieves much higher computational efficiency and yields better results in dealing with correlated

power injections than other alternatives. It should be noted that the traditional deterministic PF has been widely used for contingency analysis but the uncertainties of power injections are not considered. The developed method is able to provide lower and upper bounds of the analysis results. Thus, the risk of the contingency can be effectively quantified and appropriate control strategies can be planned, yielding greater system reliability and security.

II. PROPOSED METHOD

A. Introduction of Evidence Theory

Evidence theory is a general framework to deal with interval uncertainty, with connections to probability, possibility and imprecise probability theories [6]. It is represented by a Dempster-Shafer structure (DS) with a set of closed intervals (named focal elements) and basic probability assignment (BPA) shown as follows:

$$m : 2^\Omega \rightarrow [0, 1], \quad m(\emptyset) = 0, \quad \sum_{A \subseteq \Omega} m(A) = 1 \quad (1)$$

where Ω is the universe; 2^Ω is the power set of all subsets of Ω ; every set with a non-zero mass in 2^Ω is called a focal element. Evidence theory bounds the probability of any set (denoted by A) by intervals. Belief $Bel(A)$ is the lower bound and plausibility $Pl(A)$ represents the upper bound, yielding

$$Bel(A) \leq P(A) \leq Pl(A) \quad (2)$$

$$Pl(A) = \sum_{B \cap A \neq \emptyset} m(B) \quad Bel(A) = \sum_{B \subseteq A} m(B) \quad (3)$$

B. Joint DS of Correlated Power Injections

To consider the correlations among power injections, the joint DS is constructed based on the multidimensional ellipsoidal convex model [7]. The interval for each uncertain power injection X_i , can be expressed as:

$$X_i^I = [X_i^L \quad X_i^U] = \left\{ X_i \mid (\mathbf{X} - \mathbf{X}^0)^T \mathbf{C}^{-1} (\mathbf{X} - \mathbf{X}^0) \leq 1 \right\} \\ i = 1, 2, \dots, n \quad (4)$$

where $\mathbf{X} = [X_1, X_2, \dots, X_n]^T$; $\mathbf{X}^0 = [X_1^0, X_2^0, \dots, X_n^0]^T$ is the midpoint vector and \mathbf{C} is the covariance matrix. The midpoint

Manuscript received May 19, 2019; revised August 31, 2019, October 2, 2019, and October 3, 2019; accepted October 10, 2019. Date of publication October 16, 2019; date of current version January 7, 2020. This work was supported by The National Key Research and Development Program of China under Grant 2017YFB0902002. Paper no. PESL-00116-2019. (*Corresponding author: Qi Huang.*)

B. Liu, Q. Huang, and W. Hu are with the Mechanical and electrical engineering School and the Sichuan Provincial Key Lab of Power System Wide-area Measurement and Control, University of Electronic Science and Technology of China, Chengdu 611731, China (e-mail: liubi_2006@126.com; hwong@uestc.edu.cn; whu@uestc.edu.cn).

J. Zhao is with the Department of Electrical and Computer Engineering, Mississippi State University, Starkville, MS 39762 USA (e-mail: junbo@ece.msstate.edu).

Color versions of one or more of the figures in this article are available online at <http://ieeexplore.ieee.org>.

Digital Object Identifier 10.1109/TPWRS.2019.2947779

and covariance of X_i and X_j can be calculated via

$$X_i^0 = \frac{X_i^L + X_i^U}{2} \quad C_{ij} = \rho_{ij} \sqrt{D_i D_j} \quad i, j = 1, 2, \dots, n \quad (5)$$

where D_i and ρ_{ij} denote the variance of X_i and the correlation coefficient of variables X_i and X_j , respectively. Specifically,

$$D_i = \left(\frac{X_i^U - X_i^L}{2} \right)^2 \quad (6)$$

To obtain the joint DS of correlated power injections via ellipsoidal convex model, one must have the DS of each injection (called marginal DS). This can be achieved via the following Cartesian product D :

$$D = A_1 \times A_2 \times \dots \times A_n \\ = \left\{ d_{i_1, i_2, \dots, i_n} = [X_1^{i_1}, X_2^{i_2}, \dots, X_n^{i_n}], \right. \\ \left. X_1^{i_1} \in A_1, X_2^{i_2} \in A_2, \dots, X_n^{i_n} \in A_n \right\} \quad (7)$$

where A_i and D represent the corresponding power set of evidence variable X_i and variable vector $\mathbf{X} = [X_1, X_2, \dots, X_n]^T$; $X_1^{i_1}, X_2^{i_2}, \dots, X_n^{i_n}$ and d_{i_1, i_2, \dots, i_n} denote the focal elements of A_1, A_2, \dots, A_n and D , respectively. Without correlations, the initial joint BPA d_{i_1, i_2, \dots, i_n} is

$$BPA(d_{i_1, i_2, \dots, i_n}) = \prod_{i=1}^n BPA(X_i^{i_1}) \quad (8)$$

Thus, the initial joint DS of vector $\mathbf{X} = [X_1, X_2, \dots, X_n]^T$ can be constructed by (7) and (8). Based on this, the procedure of calculating the joint DS of correlated power injection \mathbf{X} , is developed as follows:

- 1) Construct the ellipsoidal equation according to (4)–(6):

$$G(\mathbf{X}) = (\mathbf{X} - \mathbf{X}^0)^T \mathbf{C}^{-1} (\mathbf{X} - \mathbf{X}^0) \leq 1 \quad (9)$$

- 2) Through (6), the n -dimensional cube region that is formed by the intervals of injections can be transferred to the n -dimensional ellipsoid region Ω with correlations considered. We then substitute the vertex V_{i_1, i_2, \dots, i_n} of the cube A_{i_1, i_2, \dots, i_n} formed by the focal element d_{i_1, i_2, \dots, i_n} into ellipsoidal equation (9). If the result is less than 1, it means that the vertex is inside the ellipsoid and vice versa, yielding

$$\begin{cases} G(V_{i_1, i_2, \dots, i_n}) \leq 1 & \text{inside of the ellipsoid} \\ G(V_{i_1, i_2, \dots, i_n}) > 1 & \text{outside of the ellipsoid} \end{cases} \quad (10)$$

- 3) Let $BP = 0$, if all the vertexes of the cube A_{i_1, i_2, \dots, i_n} are outside the ellipsoid $A_{i_1, i_2, \dots, i_n} \cap \Omega = \emptyset$; then let $BP = BP + BPA(d_{i_1, i_2, \dots, i_n})$ and reassign the BPA of the focal element d_{i_1, i_2, \dots, i_n} , and let $BPA(d_{i_1, i_2, \dots, i_n}) = 0$.
- 4) Obtain the joint BPA of other focal elements, which should satisfy $A_{i_1, i_2, \dots, i_n} \cap \Omega \neq \emptyset$ and

$$BPA(d_{i_1, i_2, \dots, i_n}) = \frac{BPA(d_{i_1, i_2, \dots, i_n})}{1 - BP} \quad (11)$$

where BP is the sum of BPA of all the focal elements d_{i_1, i_2, \dots, i_n} outside of the ellipsoid.

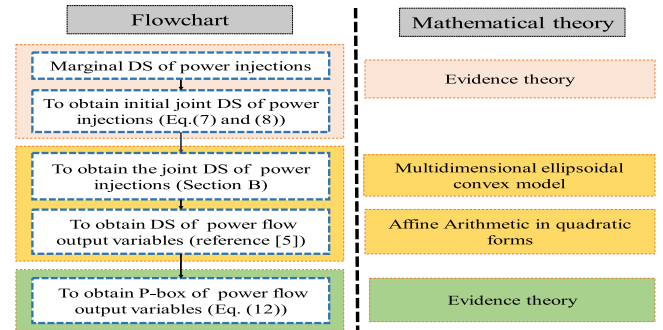


Fig. 1. The flowchart of the proposed approach.

TABLE I
CORRELATION COEFFICIENT MATRIX

Bus	Bus 13	Bus 23	Bus 27
Bus 13	1	0.8	0.6
Bus 23	0.8	1	0.75
Bus 27	0.6	0.75	1

C. DS and P-Box of Power Flow Results

The extensional Affine Arithmetic in quadratic forms can be utilized to obtain the DS of power flow outputs [5]. According to (1)–(3), if one has the DS of power flow output state variable γ , its P-box (description about the uncertainty) can be given as:

$$Bel(\gamma < x) \leq P(\gamma \leq x) \leq Pl(\gamma < x) \quad (12)$$

The flowchart of the proposed approach is shown in Fig. 1.

Remark: There have been in the last years a few works in robust optimization, particularly OPF and SCOPF [8], which compute optimal control actions to immunize operation constraints. Interval PF is usually used for contingency analysis while optimal OPF and SCOPF are for economic analysis considering the security constraints. Although their objectives and time-scales are different, the proposed method can be integrated with OPF to develop robust OPF method taking into account uncertain and correlated power injections. We will report these results in our future work.

III. CASE STUDY

A. Results on IEEE 30-Bus System

The performance of the proposed method (PM) is evaluated on the IEEE 30-bus test system with uncertain power injections. The method proposed in [5], called traditional method (TM), is used for comparison. Monte Carlo (MC) simulation results with 1000 samples are treated as the benchmark.

It is assumed three generators at buses 13, 23 and 27 are with uncertain power injections [38 66.5], [47.5 74], and [46 70] MW, respectively. Their correlation coefficient (CC) matrix is displayed in Table I. Without loss of generality, the uncertainties are assumed to be Gaussian distributed, where the mean values are the midpoints of those intervals and their variances are determined by the 3σ principle. The intervals of those variables are discretized into n uniform subintervals. The CDF obtained

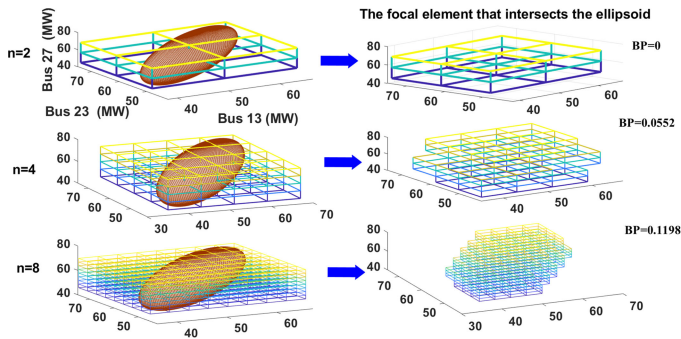


Fig. 2. Effective focal elements of joint DS.

 TABLE II
 COMPUTING TIME WITH DIFFERENT DISCRETIZATION NUMBER

Discretization numbers n	Number of focal elements		CPU time (s)		
	TM	PM	TM	PM	MC
2	8	8	0.012	0.012	8.826
4	64	42	0.11	0.066	
8	512	220	0.36	0.23	
16	4096	1271	0.73	0.40	
32	32768	7864	2.52	2.50	
64	262144	52995	5.90	3.53	

 TABLE III
 COMPUTING TIME WITH DIFFERENT CCs ($n = 6$)

CC	Number of focal elements		CPU time (s)		
	TM	PM	TM	PM	MC
0	216	192	0.212	0.21	8.74
0.6	216	132	0.22	0.17	8.73
0.8	216	84	0.22	0.13	8.74
0.98	216	36	0.22	0.021	8.73

from Monte Carlo simulation is regarded as the true CDF of the interested power flow outputs. Furthermore, the impacts of different CCs on the uncertain power flow analysis are investigated, including 0.9, 0.8, 0.6 and 0. Only the voltage magnitude (Vol. Mag) of bus 12 is shown due to the space limitation. The results are presented in Fig. 2 to Fig. 4, Table II and Table III. It can be found from Fig. 2 that the accuracy of joint DS for the power injections is improved with the increase of discretization number n . This is because, with the increase of BP, more focal elements that do not intersect with the ellipsoid are eliminated. From Fig. 3, the P-box of the Vol. Mag at bus 12 is closer to the MC CDF with larger discretization number n . This verifies that the P-box of proposed approach converges to the true CDF.

From Tables II and III, we find that both PM and TM have much higher computational efficiency than the MC method. When the discretization number n and the CCs increase, PM yields much better computational efficiency than TM as it is able to eliminate the useless focal elements outside the ellipsoid.

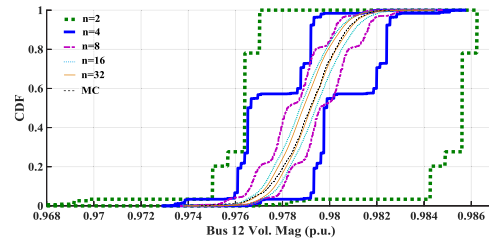


Fig. 3. P-box of bus 12 Vol. Mag with the proposed method.

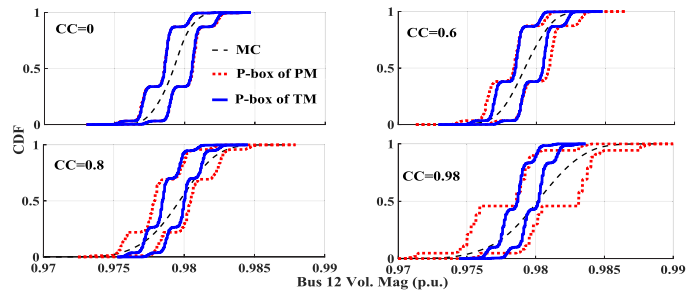


Fig. 4. P-box of Vol. Mag at bus 12 with different CCs.

Taking a closer look at Fig. 4, one can observe that the MC CDF curve tends to be more and more flat with the increase of CC, indicating that the voltage distribution becomes more and more dispersive. The P-box of TM yields poor performance in tracking the trend of the MC CDF as the correlations of uncertain power injections are not effectively accounted while PM follows that closely. Note that PM is able to take the correlations into account through the multidimensional ellipsoid convex model. It is interesting to find that P-box of PM seems to be broader than TM due to less number of focal elements. However, the results of TM are not satisfactory as it fails to capture the tails of the distribution.

B. Results on the IEEE 300-Bus System

The performance of each method is also tested on IEEE 300-bus system with varying CCs of the uncertain power injections. It is assumed that generators at buses 8, 10 and 20 and loads at buses 38, 44 and 59 are with uncertainties. Power injection intervals are assumed to be deviating from the original mean bus injection by $\pm 25\%$. The simulated CCs are 0.9, 0.8, 0.6 and 0. P-boxes of Vol. Mag at bus 40 and voltage angle (Vol. Ang) at bus 88 are depicted in Fig. 5. We find that the P-box converges to a curve in the middle (which is close to the true CDF), denoted by the average CDF curve via

$$F_A^{-1}(x) = \frac{(F_U^{-1}(x) + F_L^{-1}(x))}{2} \quad (13)$$

where $F_A^{-1}(x)$, $F_U^{-1}(x)$ and $F_L^{-1}(x)$ denote the inverse of the average CDF, upper and lower bounds of the P-box, respectively. We also find that the average CDF of PM exhibits more and more dispersive distribution as the value of CC increases. This is consistent with the changing trend of the MC CDF curve.

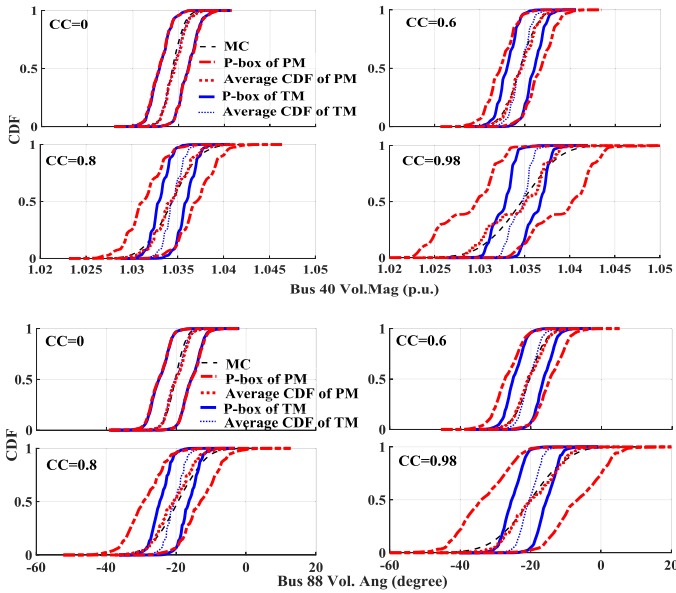


Fig. 5. P-box of power flow outputs with different CCs ($n = 4$) Upper: Bus 40 Vol. Mag and lower: Bus 88 Vol. Ang.

TABLE IV
COMPUTING TIME WITH DIFFERENT CCs ($n = 3$)

CC	Number of focal elements		CPU time	
	TM	PM	TM(hour)	PM(s)
0.6	58049 ²	1244672	65.8435	56.5280
0.7	58049 ²	982272	65.6873	45.3470
0.8	58049 ²	540672	65.4350	32.6560
0.9	58049 ²	163840	65.7466	15.3369

However, the average CDF of TM is not sensitive to the variation of CC, because it is unable to effectively deal with the correlations among the power injections.

C. Computational Assessment With Large-Scale System

To further illustrate the advantage of PM in computational efficiency, a large-scale 3120-bus system is tested whose data can be found in Matpower. The uncertain power injections are

supposed to be with generator buses 58, 59, 68, 69, 71, 91, 93, 96, 119, 120 and load buses 563, 579, 580, 582, 583, 585, 586, 587, 593, 594. The tested CCs are 0.6, 0.7, 0.8 and 0.9, respectively. The deviations of the uncertain injection from their original values are 25%. Here, the parallel computing tool with 10 workstations is applied. The computing time is shown in Table IV that validates that the developed PM achieves much higher computational efficiency than the TM, especially for strongly correlated power injections.

IV. CONCLUSIONS AND FUTURE WORK

In this paper, the multidimensional ellipsoidal convex model is integrated with the evidence theory to deal with uncertain power injections in the interval power flow. The ellipsoidal convex model allows us to effectively account for uncertain power injection correlations and eliminate irrelevant focal elements. Simulation results under various uncertain power injection levels and correlations demonstrate that the proposed method achieves higher computational efficiency and more accurate results for PF. Future work will be on the integration of the proposed approach into decision making tool and the extension of the proposed work to consider tap changer limits.

REFERENCES

- [1] C. Zhang, H. Chen, K. Shi, M. Qiu, D. Hua, and H. Ngan, "An interval power flow analysis through optimizing-scenarios method," *IEEE Trans. Smart Grid*, vol. 5, no. 9, pp. 5217–5226, Sep. 2018.
- [2] T. Ding *et al.*, "Interval power flow analysis using linear relaxation and optimality-based bounds tightening (OBBT) methods," *IEEE Trans. Power Syst.*, vol. 30, no. 1, pp. 177–188, Jan. 2015.
- [3] C. Duan, L. Jiang, W. Fang, and J. Liu, "Moment-SOS approach to interval power flow," *IEEE Trans. Power Syst.*, vol. 1, no. 32, pp. 522–530, Jan. 2017.
- [4] A. Vaccaro and A. C. Claudio, "An affine arithmetic-based framework for uncertain power flow and optimal power flow studies," *IEEE Trans. Power Syst.*, vol. 1, no. 32, pp. 274–288, Jan. 2017.
- [5] J. Luo, L. Shi, and Y. Ni, "Uncertain power flow analysis based on evidence theory and affine arithmetic," *IEEE Trans. Power Syst.*, vol. 1, no. 33, pp. 1113–1115, Jan. 2018.
- [6] T. Denoeux, "Logistic regression, neural networks and dempster-shafer theory: A new perspective," *Knowl-Based Syst.*, vol. 176, pp. 54–67, Jul. 2019.
- [7] B. Ni *et al.*, "Discussions on non-probabilistic convex modeling for uncertain problems," *Appl. Math. Model.*, vol. 59, pp. 54–85, 2018.
- [8] F. Capitanescu *et al.*, "State-of-the-art, challenges, and future trends in security constrained optimal power flow," *Elect. Power Syst. Res.*, vol. 81, no. 8, pp. 1731–1741, 2011.